Mechanisms Governing the Level of Susceptibility of Erythrocyte Membranes to Secretory Phospholipase A_2

Lauren B. Jensen,* Nancy K. Burgess,* Denise D. Gonda,* Emily Spencer,* Heather A. Wilson-Ashworth,† Erin Driscoll,* Mai P. Vu,* Jeremy L. Fairbourn,* Allan M. Judd,* and John D. Bell*

*Department of Physiology and Developmental Biology, Brigham Young University, Provo, Utah; and †Department of Biology, Utah Valley State College, Orem, Utah

ABSTRACT Although cell membranes normally resist the hydrolytic action of secretory phospholipase A_2 ($sPLA_2$), they become susceptible during apoptosis or after cellular trauma. Experimentally, susceptibility to the enzyme can be induced by loading cells with calcium. In human erythrocytes, the ability of the calcium ionophore to cause susceptibility depends on temperature, occurring best above ~35°C. Considerable evidence from experiments with artificial bilayers suggests that hydrolysis of membrane lipids requires two steps. First, the enzyme adsorbs to the membrane surface, and second, a phospholipid diffuses from the membrane into the active site of the adsorbed enzyme. Analysis of kinetic experiments suggested that this mechanism can explain the action of $sPLA_2$ on erythrocyte membranes and that temperature and calcium loading promote the second step. This conclusion was further supported by binding experiments and assessment of membrane lipid packing. The adsorption of fluorescent-labeled $sPLA_2$ was insensitive to either temperature or ionophore treatment. In contrast, the fluorescence of merocyanine 540, a probe sensitive to lipid packing, was affected by both. Lipid packing decreased modestly as temperature was raised from 20 to 60°C. Calcium loading enhanced packing at temperatures in the low end of this range, but greatly reduced packing at higher temperatures. This result was corroborated by measurements of the rate of extraction of a fluorescent phosphatidylcholine analog from erythrocyte membranes. Furthermore, drugs known to inhibit susceptibility in erythrocytes also prevented the increase in phospholipid extraction rate. These results argue that the two-step model applies to biological as well as artificial membranes and that a limiting step in the hydrolysis of erythrocyte membranes is the ability of phospholipids to migrate into the active site of adsorbed enzyme.

INTRODUCTION

Secretory phospholipase A_2 ($sPLA_2$) has been studied for many years as a model for the action of an enzyme at a lipid/water interface. Several investigations have suggested that the action of the enzyme on membrane surfaces requires two steps (Scheme 1, reviewed in Gelb et al., 1995; Jain and Berg, 1989). The first step consists of adsorption of $sPLA_2$ to the membrane surface. The second step involves binding of phospholipid molecules in the active site of the adsorbed enzyme (Gelb et al., 1995; Jain and Berg, 1989; Bell and Biltonen, 1989). The second step also has a direct requirement for calcium as a cofactor and can be inhibited by replacing calcium with barium (Dam-Mieras et al., 1975; Yu et al., 1993a, 1998). Either or both steps may be limiting for artificial bilayers that are resistant to $sPLA_2$, but certain perturbations to membrane structure, such as increased microheterogeneity or negative charge at the membrane surface, overcome such limitations (Jain et al., 1989; Burack and Biltonen, 1994; Honger et al., 1996; Henshaw et al., 1998; Yu et al., 2000; Tatulian, 2001; Bezzine et al., 2002).

We propose that the action of $sPLA_2$ on biological membranes involves the same two steps. Normally, cell membranes resist hydrolysis by the enzyme (Smith et al., 2001; Wilson et al., 1999; Nielson et al., 2000). However, under certain conditions, such as during apoptosis or after cellular trauma, they become highly susceptible (Smith et al., 2001; Wilson et al., 1999; Judd et al., 2003; Nielson et al., 2000; Atsumi et al., 1997). We have used human erythrocytes as a model to study the factors governing membrane susceptibility to $sPLA_2$ (Vest et al., 2004; Smith et al., 2001; Harris et al., 2001; Best et al., 2002). Experimentally, loading the cells with calcium via an ionophore can induce susceptibility to the enzyme. This effect of calcium is indirect and separate from its role as a catalytic cofactor as described above. Apparently, this indirect effect of calcium involves changes in membrane physical properties that lead to an increase in the extent of boundaries between domains of ordered and disordered lipids (Vest et al., 2004; Smith et al., 2001; Harris et al., 2001; Best et al., 2002). The hypothesis was proposed that phospholipid-neighbor interactions are weakened at these boundaries, allowing phospholipids in those regions to migrate from their normal position in the bilayer into the enzyme active site (Best et al., 2002; Smith et al., 2001).

To test this hypothesis more explicitly, we have examined two predictions that should occur when the membrane is susceptible: the second step in the hydrolysis scheme should be enhanced, and the packing of membrane lipids at domain boundaries should be reduced. These predictions were explored with kinetic measurements of membrane hydrolysis, assessment of membrane adsorption by fluorescent-labeled

Submitted November 20, 2004, and accepted for publication January 21, 2005.

Address reprint requests to John D. Bell, Tel.: 801-422-2353; Fax: 801-422-0050; E-mail: john_bell@byu.edu.

0006-3495/05/04/2692/14 $2.00

doi: 10.1529/biophysj.104.056457

$$E + M_S \overset{K_1}{\rightleftharpoons} E_B \overset{K_2\,S,\ \mathrm{Ca}^{2+}}{\rightleftharpoons} E_B{}^S \xrightarrow{k_{cat}} E_B + P$$

SCHEME 1 Reaction scheme for the interaction of $sPLA_2$ with cell membranes. E, $sPLA_2$; E_B, $sPLA_2$ adsorbed to available sites (M_S) on the membrane surface; S, substrate (membrane phospholipid); E_B^S, active enzyme ($sPLA_2$ adsorbed to the membrane surface with phospholipid bound to the active site); k_{cat}, rate constant of hydrolysis; P, product.

$sPLA_2$, and by the fluorescence of two probes: merocyanin 540 (MC540) and a fluorescent phospholipid analog, 2-(6-(7-nitrobenz-2-oxa-1 3-diazol-4-yl)amino)hexanoyl-1-hexadecanoyl-*sn*-glycero-3-phosphocholine (NBD-PC). MC540 binds to the outer leaflet of cell membranes (Sieber, 1987) and detects subtle differences in membrane packing revealed by a 20-nm red-shift in emission maximum as lipids become less tightly packed (Langner and Hui, 1993; Stillwell et al., 1993; Yu and Hui, 1992). NBD-PC has been used extensively to study the behavior of membrane phospholipids (reviewed in Chattopadhyay, 1990) and functions as a substrate for $sPLA_2$ (Meyuhas et al., 1992).

MATERIALS AND METHODS

Reagents

Erythrocytes were obtained from individuals receiving blood tests during physical examinations at the Brigham Young University Student Health Center, stored overnight at 4°C and prepared for experiments in modified balanced salt solution (MBSS; 134 mM NaCl, 6.2 mM KCl, 1.6 mM $CaCl_2$, 1.2 mM $MgCl_2$, 18 mM HEPES, 13.6 mM glucose, pH 7.4 at 37°C) as explained previously in Smith et al. (2001).

Active monomeric aspartate 49 $sPLA_2$ and the inactive lysine 49 form (AppK49) from the venom of *Agkistrodon piscivorus piscivorus* were isolated according to the published procedure of Maraganore et al. (1984). Prior studies have verified that this enzyme behaves qualitatively the same as human groups IIa and V $sPLA_2$ in the types of experiments described in this report (Wilson et al., 1999; Smith et al., 2001). Stock solutions of the enzyme (0.1 to 1.2 mg/ml) were prepared in 50 mM KCl with 3 mM NaN_3 and stored at 4°C.

Ionomycin was purchased from Calbiochem (La Jolla, CA) and dissolved in dimethylsulfoxide (DMSO) for experiments. Control experiments using DMSO instead of ionomycin demonstrated that the solvent had no effect on the experimental results reported in this article or on cell morphology or membrane physical properties (assessed by two-photon microscopy). The DMSO concentration in samples after addition of ionomycin was 0.25% (v/v). Furthermore, controls in which calcium in the cell medium had been replaced with EDTA demonstrated that fluorescence measurements of membrane properties were due to calcium entry into the cell rather than artifacts resulting from direct effects of ionomycin on cell membranes.

NBD-PC and MC540 were obtained from Molecular Probes (Eugene, OR). Bovine serum albumin (BSA; 96–99%, fraction V) was purchased from Sigma (St. Louis, MO). R5421 was a gift of Jeffrey T. Billheimer at Dupont Merck Pharmaceutical (Wilmington, DE). Other reagents were obtained from standard sources.

Merocyanine 540 fluorescence

Emission spectra of MC540 were acquired (emission, 550–700 nm; excitation, 540 nm, 4–16 nm bandpass, depending on sample intensity) with a Fluoromax (Jobin Yvon Horiba, Edison, NJ) or PC-1 (ISS, Champaign, IL) photon-counting spectrofluorometer at temperatures ranging from 20.0 to 60.0°C. Sample homogeneity was maintained by continuous gentle stirring with a magnetic stir bar. MC540 (0.3 μM final) was added to 2 ml MBSS in a fluorometer sample cell and incubated for 5 min at the desired temperature before obtaining an initial spectrum as an aqueous reference. Washed erythrocytes (final density of $\sim$3–4 $\times$ 10^6 cells/ml) were then added to the sample, and a second emission spectrum was acquired after sufficient time had passed for the MC540 to reach equilibrium with the cells (varying from 5 to 20 min, depending on the temperature). Ionomycin (300 nM final) was finally added, and a third spectrum was attained after 10 min. Difference spectra were calculated by subtracting the aqueous reference spectrum from each of the spectra obtained in the presence of cells (i.e., both before and after ionomycin treatment).

Membrane hydrolysis by $sPLA_2$

Release of free fatty acids from erythrocytes was assayed with ADIFAB (65 nM final; excitation, 390 nm; emission, 432 nm and 505 nm) as described in Harris et al. (2001) and Richieri and Kleinfeld (1995). Washed erythrocytes were suspended as in the experiment with MC540. After initiating data acquisition, ADIFAB was added at 30 s, followed by ionomycin (300 nM) or DMSO at 130 s, and $sPLA_2$ (21−700 nM) at 730 s. Hydrolysis results were quantified by calculating the generalized polarization (GP) and estimating the initial hydrolysis rate at the 20-s time point by nonlinear regression as described in Harris et al. (2001).

Two-photon excitation scanning microscopy

Scanning two-photon excitation microscopy images were collected on an Axiovert 35 inverted microscope (Zeiss, Thornwood, NY) with temperature control at the Laboratory for Fluorescence Dynamics (Urbana, Il), as described previously in Harris et al. (2001), Smith et al. (2001), and Yu et al. (1996). Laser emission was 780 nm at 70–100 mW for fluorescamine experiments and 940 nm at 35–40 mW for NBD-PC.

Phospholipid extraction

NBD-PC was incorporated into the cell membrane using a modified protocol of Williamson et al. (1992). NBD-PC (dissolved in ethanol) was dried by evaporation with nitrogen gas in a glass test tube. An appropriate volume of MBSS (generally 1–3 ml) was added to the tube, and the dried film of NBD-PC (13 μM, final) was suspended by vigorous agitation on a vortex mixer. Three parts of this suspension was incubated with one-part washed erythrocytes (3–4 $\times$ 10^7 cells/ml final, $\sim$2 $\times$ 10^8 NBD molecules/cell) for 30 min in the dark at ambient temperature. After incubation, cells were washed again and resuspended in 2 ml fresh MBSS at a density of 3–4 $\times$ 10^6 for experiments.

Phospholipid release was assayed by fluorescence spectroscopy using BSA or $sPLA_2$ as the phospholipid acceptor (see above for fluorometer details). NBD-PC-labeled cells were incubated for 5 min at temperatures indicated in Figs. 6–12 before initiating acquisition of the fluorescence emission intensity (excitation, 485 nm; emission, 535 nm). Either ionomycin (300 nM final) or an equivalent volume of the solvent, DMSO, was added at 120 s.

For extraction with BSA, 150 μl of 10% BSA (0.7% final) was added at 720 s, and the data were fit to the following equation by nonlinear regression starting from the time of addition of BSA,

$$Y = A(1 - e^{-Bt}) + C(1 - e^{-Dt}) + I, \qquad (1)$$

where A and C represent the magnitude of fluorescence change and B and D are the rate constants for slow and fast components of change. Control experiments adding BSA to samples of unlabeled erythrocytes or erythrocytes from which NBD-PC had already been extracted were used to assess artifacts caused by dilution or optical changes contributed by the BSA addition. The intercept I accounted quantitatively for these artifacts. Data are expressed as a normalized derivative evaluated at $t = 0$ s:

$$\frac{dY}{dt_0} = \frac{AB + CD}{Y_{300}}. \quad (2)$$

Y_{300} is the total amount of fluorescence change evaluated at 300 s (i.e., at steady state). Some experiments included various drugs with known effects on the ability of $sPLA_2$ to hydrolyze erythrocyte membranes. For high KCl treatment, normal MBSS was replaced in all steps with MBSS containing 89 mM KCl and 51 mM NaCl. EDTA treatments used MBSS containing 20 mM EDTA in lieu of calcium. For trials with the scramblase inhibitor, R5421 (50 μM final) was added to the samples incubating in the fluorometer 10 min before either DMSO or ionomycin. Phenylhydrazine (freshly dissolved in DMSO before each experiment; 0.5 mM final) was added to samples immediately before DMSO or ionomycin.

For extraction with $sPLA_2$, 20 μl of 7 μM $sPLA_2$ was added at 720 s (70 nM, final) instead of BSA. In this case, no optical artifact occurred upon addition of the enzyme. The data were fit by nonlinear regression to Eq. 15 (Results).

Secretory PLA_2 adsorption to erythrocytes

$sPLA_2$ was labeled with fluorescamine by incubating the enzyme (1.4 μM) in 2 ml MBSS with 34 μl of a 3 mg/ml stock solution of fluorescamine dissolved fresh in acetone. Control experiments in which additional unlabeled enzyme was added verified that labeling was complete under these conditions after the fluorescence intensity (excitation, 390 nm; emission, 485 nm) had increased to a stable level (~10 min). Washed erythrocytes were suspended in MBSS in which $CaCl_2$ and $MgCl_2$ were replaced with 2 mM $BaCl_2$ to allow enzyme adsorption to the membrane surface but impair membrane hydrolysis (Dam-Mieras et al., 1975; Yu et al., 1993a, 1998). In experiments testing the effect of ionomycin, cells were suspended in normal MBSS to which 20 mM $BaCl_2$ was added to prevent hydrolysis but still allow calcium to enter the cell and cause the membrane changes associated with susceptibility. Control experiments revealed that these two expectations were met under our conditions. Additional controls testing the ability of fluorescamine-labeled $sPLA_2$ to hydrolyze erythrocytes with or without ionomycin treatment demonstrated that the behavior of the labeled enzyme was comparable to the native protein.

Adsorption was assayed by either two-photon microscopy or a centrifugation assay. For two-photon microscopy, 1 ml of erythrocytes (3–4 $\times$ 10^6/ml) was equilibrated with ionomycin (300 nM) or equivalent DMSO for at least 5 min. Baseline images were then acquired to account for cell intrinsic fluorescence. Labeled $sPLA_2$ (67 or 130 nM final) was added to samples and additional images were acquired. In some cases, repeated images of the same field were acquired before and after enzyme. This method had the advantage of assessing repeatedly the intensity of the same cells. However, repeated exposure to the laser led to elevated cell autofluorescence. This autofluorescence was quantified and subtracted from the data. Since this effect could represent laser-induced damage to cells, we also repeated the experiment using images of different fields of cells to avoid this potential difficulty. This second method produced data with more variation (because more fields were assessed), but the results were comparable to those obtained repeatedly from the same field without the problem of autofluorescence. Experiments from both protocols were pooled for the statistical analysis of adsorption described in the text. Finally, some experiments included unlabeled $sPLA_2$ (1.0–2.5 μM active or AppK49) added either before or after labeled enzyme to test for the ability of the enzymes to compete for adsorption.

Quantitative analysis involved assessing the increase in image fluorescence intensity after addition of labeled $sPLA_2$. The contribution of laser-exposure-dependent autofluorescence in multiple images of the same field was estimated by linear regression of image intensity during four consecutive acquisition sessions before addition of labeled $sPLA_2$. The regression line was then extrapolated to the fifth session, which was acquired after enzyme addition. This extrapolated intensity was used as the blank to be subtracted from the data. When images before and after addition of labeled enzyme involved different fields, the fluorescence intensity was assessed for each individual cell in the fields. The difference in average intensity per cell was then calculated for the images before and after enzyme exposure.

Cells were similarly prepared and incubated with DMSO or ionomycin for the centrifugation assay. In this case, samples were treated in microcentrifuge tubes instead of microscopy dishes. Also, cell (6–7 $\times$ 10^6/ml), labeled-enzyme (130 nM), and ionomycin (550 nM) concentrations were increased to improve signal size. Labeled $sPLA_2$ was then added, and the incubation continued for 10 min at the experimental temperature. Cells were then isolated by rapid centrifugation (15 s at 13,000 $\times$ g), washed in 1 ml ice-cold MBSS, and centrifuged again. The supernatant was discarded, and the pellet suspended in 2 ml fresh MBSS and the fluorescence intensity assessed at 25°C by fluorescence spectroscopy (excitation, 390 nm; emission, 400–600 nm). Blank samples contained cells without labeled $sPLA_2$, and the total signal was determined from an aliquot of the original supernatant. Results were analyzed by subtracting the intensity of blank samples from those containing labeled enzyme. These were then compared to the total signal to ascertain the percentage of enzyme adsorbed.

Statistical analysis

In all summaries of multiple replicates, the data are expressed as the mean $\pm$ SE. Matched-pair t-tests were performed on each treatment pairing the trials that used blood from the same donor; otherwise unpaired t-tests were used. All t-tests were two-tailed. Multiple comparisons were conducted using analysis of variance. Trends were analyzed by linear regression. In every case, the null hypothesis was rejected when $p < 0.05$.

MODEL

The model describing the action of $sPLA_2$ on the surface of membranes is shown in Scheme 1. The rate of hydrolysis (dP/dt) is given by

$$\frac{dP}{dt} = k_{cat}E_B^S. \quad (3)$$

Experiments were conducted in which the concentration of cells and, therefore, the total number of adsorption sites for the enzyme (M_{ST}) were kept constant. The equilibrium constants (K_1 and K_2) are defined as

$$K_1 = \frac{E_B}{(E)(M_S)}, \quad (4)$$

$$K_2 = \frac{E_B^S}{(E_B)(S)}. \quad (5)$$

If we confine our analysis to the initial part of the hydrolysis time course, then S can be assumed to be a constant mole fraction of M_{ST} (S_0). Since S_0 is a constant, we can define an apparent equilibrium constant (K_2') that is proportional to K_2 and can be used in our calculations as

$$K_2' = \frac{E_B^S}{E_B}. \quad (6)$$

The distribution of membrane binding sites between occupied and unoccupied states is given by

$$M_{ST} = M_S + E_B + E_B^S. \quad (7)$$

If we assume that only a small fraction of added enzyme adsorbs to the cell surface, then E can be approximated by

the total enzyme concentration, E_T. The validity of this assumption was verified by binding experiments described below. An explicit description of the initial hydrolysis rate can be obtained by combining Eqs. 3, 4, 6, 7, and 8, as

$$\frac{dP}{dt} = \frac{\alpha E_T K_1 K_2'}{1 + E_T K_1 + E_T K_1 K_2'}, \quad (8)$$

where α is the apparent hydrolysis rate constant expressed in units of ADIFAB GP and is proportional to $k_{cat}\, M_{ST}$.

RESULTS

Hydrolysis kinetics

Contributions of the two steps in Scheme 1 can be distinguished by varying enzyme concentration and measuring the initial rate of hydrolysis (see Eq. 8). Fig. 1 *A* displays the results of that experiment. The hydrolysis rate of cellular membranes increased significantly upon loading the cells with calcium using the ionophore ionomycin (*triangles*). This increase in rate was apparent at all $sPLA_2$ concentrations: a two-way analysis of variance estimated that treatment with ionomycin accounted for 34.3% of the total variation ($p < 0.0001$) and increasing the enzyme concentration accounted for 14.1% of the total variation ($p = 0.008$). Statistical interaction between the two variables was not significant ($p = 0.76$).

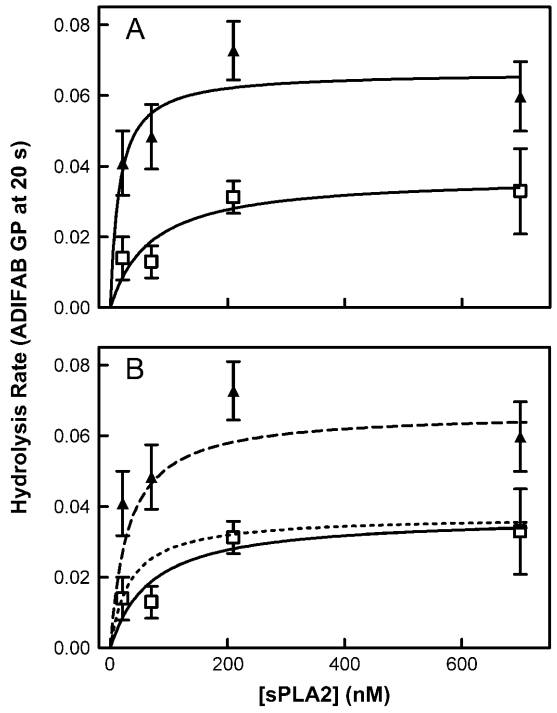

FIGURE 1 Effect of ionomycin treatment on the enzyme-concentration dependence of the initial rate of hydrolysis of erythrocytes. (*A*) Various concentrations $sPLA_2$ were added to ionomycin-treated (*triangles*) or control (DMSO-treated) erythrocytes (*squares*) and the initial rate of hydrolysis assessed at 37°C as explained in Materials and Methods. Each datum represents the mean ± SE of data from five to seven blood samples. The curves represent global nonlinear regression of the data using Eq. 8. In *A*, the value of α was held constant, and K_1 and K_2' were allowed to vary (values summarized in Table 1). In *B*, the components of the fit for ionomycin-treated samples in *A* were altered individually from control values. (*Solid curve*, same fit for control samples as in *A*; *dotted curve*, the value of K_1 was increased by a factor of 2; *dashed curve*, the value of K_2' was increased by a factor of 4.)

Equation 8 was used in a global nonlinear regression analysis of the data collected for Fig. 1 *A*. We assumed that α (i.e., representative of k_{cat}) was not dependent upon membrane changes provoked by ionomycin reasoning that once a phospholipid has moved out of the membrane and into the active site of the enzyme, it is no longer affected by the membrane properties that determine susceptibility. We, therefore, constrained α to remain equal between the two conditions (ionomycin-treated cells and control cells). Table 1 shows the results of the global analysis. Changing the membrane properties by increasing intracellular calcium amplified the equilibrium constant for the first step (K_1) by a factor of 2 and the equilibrium constant for the second step (K_2') by a factor of 4. In other words, the affinity of $sPLA_2$ for the cellular membrane doubled and the probability of a phospholipid moving into the active site of the enzyme quadrupled. Because K_1 is a second-order equilibrium constant and K_2' is a pseudo-first-order constant, an increase in the latter by a factor of 4 contributes much more quantitatively to the results of Fig. 1 *A* than does the doubling of the adsorption constant. Fig. 1 *B* illustrates this observation by displaying the effects of increasing each step separately. The solid curve indicates the initial hydrolysis rate of control cells (*squares*); an increase in the value of K_1 by the factor of 2 is indicated by the dotted line; an increase of K_2' by a factor of 4 is indicated by a dashed line. Clearly, the change in K_2' explained the majority of the effect of ionomycin treatment on the susceptibility of the erythrocytes to $sPLA_2$.

This analysis assumed that the same total amount of substrate was accessible to the enzyme under all experimental conditions. This assumption was validated by experiments in which cells were incubated with the enzyme for up to 10,000 s. After these extensive incubation periods, it was clear that the same amount of substrate was hydrolyzed regardless of enzyme concentration or ionomycin treatment (not shown). Thus, the effect of ionomycin on erythrocytes was to enhance the rate of hydrolysis rather than the amount of substrate available.

TABLE 1 Values of constants from Eq. 8 as obtained for nonlinear regressions in Figs. 1 and 2

Condition	Parameter values		
	α (GP/s^{-1})	K_1 (μM^{-1})	K_2'
22.6°C, ionomycin (Fig. 2)	0.0027	6.8	0.94
37.0°C, DMSO (Fig. 1)	0.0045	8.5	0.71
37.0°C, ionomycin (Fig. 1)	0.0045	17.5	2.89
43.5°C, ionomycin (Fig. 2)	0.0048	4.0	5.17

The ability of ionomycin to cause membrane changes and induce susceptibility to $sPLA_2$ has been shown to be temperature-sensitive, with mechanistic significance attributed to that sensitivity (Best et al., 2002). Accordingly, we repeated the experiment of Fig. 1 using erythrocytes treated with ionomycin at low (22.6°C) and high (43.5°C) temperature (Fig. 2 *A*). The effects of enzyme concentration (24.2% of the variation, $p < 0.0001$) and temperature (66.6% of the variation, $p < 0.0001$) were both significant by two-way analysis of variance. In this case, a significant interaction was observed between the variables (5% of the variation, $p = 0.006$), suggesting that both the height and shape of the curve were influenced by temperature. For analysis of these data, we did not assume that α would be constant. In fact, we expected α to increase with temperature due to the activation energy ($\Delta G^{\ddagger}$) of the catalytic step according to the Arrhenius equation (R is the gas constant and T is absolute temperature):

$$\frac{\alpha_2}{\alpha_1} = \exp\left[-\frac{\Delta G^{\ddagger}}{R}\left(\frac{1}{T_2} - \frac{1}{T_1}\right)\right]. \quad (9)$$

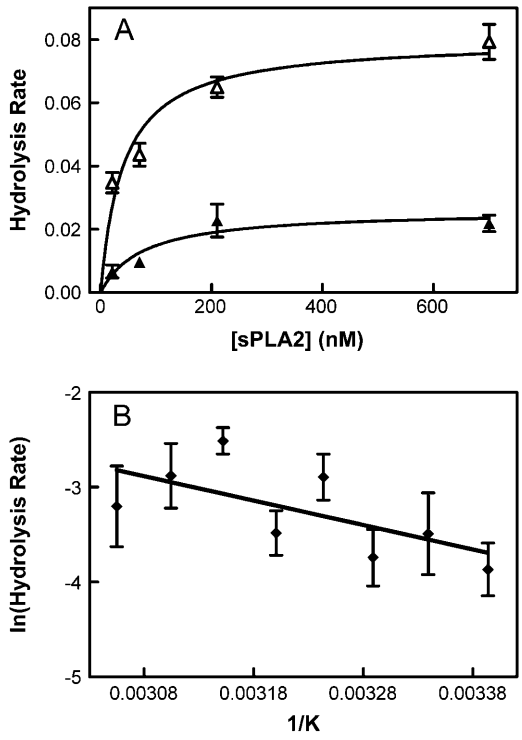

FIGURE 2 Effect of temperature on the enzyme-concentration dependence of the initial rate of hydrolysis of ionomycin-treated erythrocytes. (*A*) The experiment of Fig. 1 was repeated for ionomycin-treated samples at 22.6°C (*solid triangles*) or 43.5°C (*open triangles*). Each datum represents the mean ± SE of three separate blood samples. (*B*) The hydrolysis of 1 mM dioctanoylphosphatidylcholine micelles (*cmc* = ~0.3 mM; Heerklotz and Epand, 2001) was assessed using the same methodology as described for erythrocyte hydrolysis (70 nM $sPLA_2$). Each datum represents the mean ± SE of 3–5 samples. The temperatures indicated are the average of the actual sample temperatures for each point (all within ±2.5°C).

To estimate the activation energy independent of the effects of membrane physical changes, we assayed the temperature-dependence of hydrolysis of a short-chain substrate that forms micelles rather than bilayers. Furthermore, we conducted the experiments at substrate concentrations well above the critical micelle concentration to avoid temperature effects on micelle-monomer equilibrium. Fig. 2 *B* displays an Arrhenius analysis of the hydrolysis of the short-chain substrate. The apparent positive slope in the data among the first three data points (54.3–44.3°C) was not defensible statistically, and we therefore chose to analyze the entire data set as a single unit by linear regression. This assumption of a monotonic relationship is further justified by the observation that the enzyme does not appear to lose activity or denature until well above temperature range in Fig. 2 (Honger et al., 1996; Best et al., 2002; Singh and Chang, 2004). The activation energy from this analysis was 5.1 ± 2.2 kcal/mol, suggesting that the value of α should increase by a factor of 1.78 between 22.6 and 43.5°C based on Eq. 9. This increase in hydrolysis rate due to the apparent activation energy was insufficient to account for the fourfold enhancement of activity displayed in Fig. 2 *A*. Accordingly, to ascertain the source of the additional temperature dependence, a global analysis was conducted using the same method as in Fig. 1 but accounting for the 1.78-fold change in α. As illustrated in Table 1, the primary residual effect of temperature on hydrolysis rate was an increase in the value of K_2' (in fact, the value of K_1 actually decreased in the analysis).

The temperature data with erythrocytes summarized in Fig. 2 and Table 1 represented only samples treated with ionomycin. To ascertain whether the temperature-dependence described by these data sets applied solely to the effect of ionomycin, we repeated the analysis with control samples. At the same two temperatures, the rate of hydrolysis of control samples increased by a factor of 1.42 at 70 nM $sPLA_2$ and 1.65 at 700 nM (not shown). These results demonstrated that all of the temperature-dependence in hydrolysis rate observed in the absence of ionomycin was due to the activation energy. Thus, the complete effect of temperature on erythrocyte sensitivity to $sPLA_2$ can be explained by activation energy plus the temperature-dependence of the action of ionomycin. This result supports a hypothesis proposed previously by Best et al. (2002).

Adsorption of $sPLA_2$ to the membrane surface

The results of the kinetic analysis suggested that effects of temperature and calcium loading on the first step, enzyme adsorption to the membrane, were minimal. We sought additional evidence regarding that observation by attempting to assess directly the adsorption of the enzyme to the cell surface. Such experiments are complicated by the fact that not all adsorption visualized experimentally necessarily represents productive binding that can produce hydrolysis.

An extreme example is the fact that the enzyme can bind to membrane carbohydrates and protein receptors (Ancian et al., 1995; Koduri et al., 1998). Nevertheless, our sole objective was to determine whether ionomycin treatment and/or temperature altered adsorption to the membrane; thus, we felt justified in proceeding, notwithstanding this caveat.

To study the adsorption of $sPLA_2$ to the cellular membrane, we labeled the enzyme with fluorescamine, a fluorescent probe that covalently binds to primary amines (Udenfriend et al., 1972). Fig. 3 illustrates two-photon fluorescence microscopy images of erythrocytes before and after adding fluorescamine-labeled enzyme under conditions at which step 2, and thus hydrolysis, was inhibited (in the presence of barium (Dam-Mieras et al., 1975; Yu et al., 1993a, 1998). The fluorescence intensity did not decrease after adding unlabeled enzyme (Fig. 3 *C*), indicating either that desorption of $sPLA_2$ from the cellular membrane was very slow or that the enzyme bound nonspecifically. To distinguish these possibilities, we reversed the order of addition: unlabeled $sPLA_2$ was added before fluorescamine-labeled $sPLA_2$ (Fig. 3 *D*). A similar result was obtained when we added unlabeled AppK49 $sPLA_2$ before labeled enzyme (not shown, results same as shown in Fig. 3 *D*). Since labeled $sPLA_2$ appeared unable to bind in the presence of unlabeled enzyme, we concluded that the first possibility was more likely: the observed adsorption of $sPLA_2$ to cell membranes was long-lived but specific.

The experiment of Fig. 3 was repeated multiple times on cells treated with ionomycin or control vehicle (DMSO) at 37°C. The concentration used in these experiments (67 nM) was selected based on the kinetic results in Fig. 1 to optimize potential sensitivity to ionomycin treatment while maintaining a signal sufficiently large to measure. We assumed that if ionomycin treatment caused either a large change in binding affinity or the number of adsorption sites, the difference would be apparent at this concentration. The results were quantified as described in Materials and Methods. The measured adsorption was statistically significant in both cases (DMSO, $23 \pm 10\%$ increase in fluorescence intensity, $p = 0.04$, $n = 14$; ionomycin, $27 \pm 6\%$, $p = 0.0003$, $n = 15$, one-sample *t*-tests) but were indistinguishable from each other ($p = 0.74$, unpaired *t*-test).

Since the data of Fig. 3 suggested that enzyme desorption from the membrane surface was slow, we decided that a centrifugation assay for adsorption could also be used in an attempt to obtain data from bulk samples and allow analysis at multiple temperatures. Repetition of the experiments described in the previous paragraph with the centrifugation assay validated the result that ionomycin treatment had no effect on measured enzyme adsorption (not shown). Fig. 4 displays the temperature-dependence of enzyme adsorption using the same assay (without ionomycin). Although the temperature groups were distinguishable statistically ($p = 0.04$ by analysis of variance), no consistent trend with temperature was observed. The apparently anomalous data at

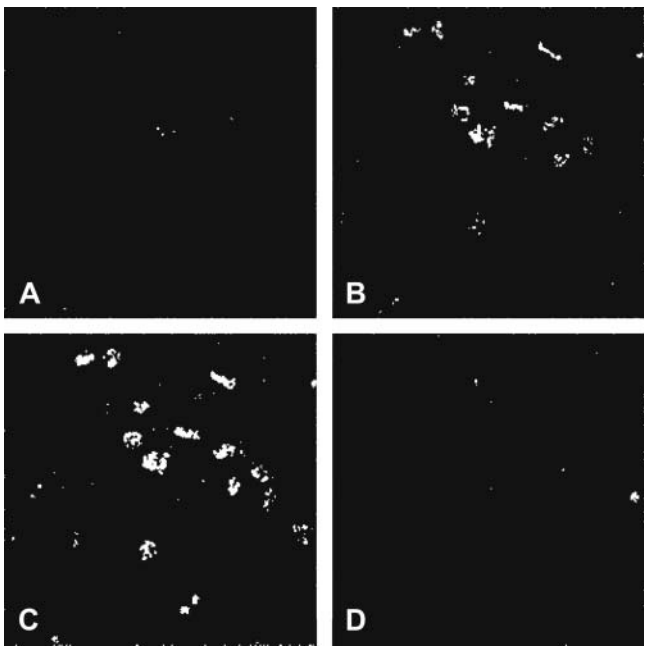

FIGURE 3 Adsorption of fluorescamine-labeled $sPLA_2$ to erythrocytes at 37°C. The experimental details of the two-photon microscopy and sample preparation are explained in Materials and Methods. The images were acquired before addition of labeled enzyme (*A*), 6 min after addition of 130-nM labeled $sPLA_2$ (*B*, same field as *A*), 4 min later and 1 min after further addition of 2.5 μM unlabeled $sPLA_2$ (*C*, same field as *B*). *D* is the image of a fresh sample of erythrocytes 10 min after addition of 2.5-μM unlabeled enzyme, which was added 9 min before 130-nM labeled enzyme.

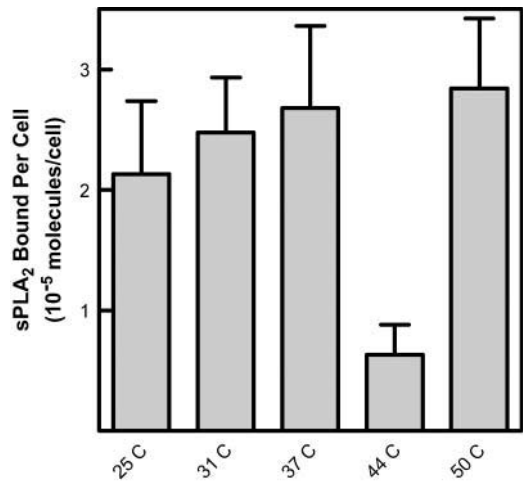

FIGURE 4 Effect of temperature on the adsorption of fluorescamine-labeled $sPLA_2$ to erythrocytes. The adsorption of 130-nM labeled $sPLA_2$ to erythrocytes was assayed by the centrifugation procedure described in Materials and Methods at the indicated temperatures. The adsorption signals in all five groups were significant ($p < 0.04$, $n = 10$, one-sample *t*-tests). One-way analysis of variance comparing the groups was significant ($p = 0.04$), although a Bonferoni post-test was unable to detect specific differences between any pairs of temperature groups.

44°C appeared to be entirely responsible for the statistical significance. Even if this group was ignored, no statistically significant trend was observed among the remaining data ($p = 0.39$ by linear regression and $p = 0.84$ by analysis of variance). We were unable to identify any explanation for the 44°C data other than experimental variation. Taken together, the adsorption data appeared to corroborate our conclusion from the global analysis of hydrolysis kinetics that changes in K_1 provoked by calcium loading or temperature were minimal.

The centrifugation assay allowed one additional benefit; an opportunity to estimate the approximate number of enzyme adsorption sites. The total potential number of binding sites was determined by dividing the total surface area of an erythrocyte by the surface area of the enzyme and suggested that 8.5×10^6 enzymes would be bound per cell if the surface were completely covered (Evans and Fung, 1972; Arni and Ward, 1996). The average number of enzymes adsorbed in all of our experiments at 130 nM $sPLA_2$ was $2.0 \pm 0.3 \times 10^5$ sites/cell. Based on the data of Figs. 1 and 2, ~70% of the potential binding sites are occupied at that concentration. Thus, at full occupancy, $sPLA_2$ was estimated to cover ~3% of the erythrocyte surface. This estimate seemed reasonable based on a semiquantitative observation from the two-photon microscopy. As a reference for comparison of the fluorescence intensity, we labeled erythrocytes directly with fluorescamine. This manipulation presumably labeled all membrane proteins. The intensity of cells thus labeled was ~20-fold greater than that of adsorbed $sPLA_2$ corroborating the conclusion that the enzyme adsorbs to only a fraction of the cell membrane surface at saturation. These results also served to validate the assumption that $E = E_T$ in the derivation of Eq. 8 (with 4×10^6 cells per sample, <2% of added enzyme molecules adsorbed to the cells at 130 nM).

Membrane lipid packing

If ionomycin treatment increases the ability of phospholipids to migrate into the enzyme active site as suggested by the kinetic results, it should decrease lipid packing, but only at higher temperatures. We first tested this prediction of the hypothesis using MC540 fluorescence. One challenge in using MC540 with erythrocytes is that the probe does not bind very well to the cell membrane (Lagerberg et al., 1995). We overcame this challenge by obtaining three consecutive spectra with each sample, one with aqueous MC540, one after addition of and equilibration with, erythrocytes (~10–20 min, depending on temperature), and one after addition of ionomycin or DMSO. Data were analyzed as difference spectra; the aqueous spectrum was subtracted from the spectrum obtained after addition of erythrocytes and also from the spectrum after addition of ionomycin or DMSO at each temperature (hemoglobin absorption of light appeared not to interfere at the wavelengths relevant to MC540). The data were gathered using this method instead of prelabeling and washing the cells before obtaining a spectrum as done in previous studies because of the rapid dissociation of the dye from the membrane after the washing step (Lagerberg et al., 1995).

The difference spectra revealed peaks at 567 nm and 587 nm. The ratio of intensity at 567–587 was calculated for erythrocytes before and after treatment with ionomycin. As expected, elevation of temperature reduced the level of lipid packing as shown by a modest reduction in the ratio of intensity at 567–587 nm (not shown). The greatest temperature sensitivity resided between 30 and 45°C, consistent with previous observations with the fluorescent probe laurdan (Best et al., 2002). Treatment of erythrocytes with ionomycin further affected the apparent degree of packing as a function of temperature (Fig. 5). At low temperatures, ionomycin treatment caused the ratio of 567:587 nm to be higher than the control, indicative of increased packing. However, at high temperature, the apparent level of packing was greatly reduced by ionomycin treatment.

Lipid packing was further examined by considering the ability of BSA to extract fluorescent phospholipids from the erythrocyte membranes. As shown in Fig. 6 *A*, the fluorescence intensity of NBD-PC was distinguishable depending on whether the probe was present as an aqueous suspension, incorporated into cell membranes, or bound to BSA. Consequently, addition of BSA to a suspension of cells labeled with NBD-PC resulted in a time-dependent increase in fluorescence intensity (Fig. 6 *B*). Control experiments using fluorescence microscopy revealed that the addition of BSA truly resulted in extraction of NBD-PC from cell membranes (Fig. 7; note that the cells had been previously washed to remove probe superficially adsorbed). Experiments in which BSA was added in the absence of NBD-PC demonstrated that ~10% of the initial increase in apparent fluorescence intensity was an optical artifact that we were able to quantify and subtract during the process of data

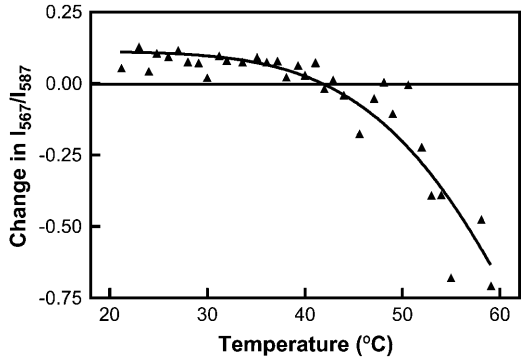

FIGURE 5 Effect of ionomycin treatment on the temperature-dependence of MC540 fluorescence in erythrocytes. The ratio of intensity at 567 nm to intensity at 587 nm was calculated from difference spectra obtained from samples before and after ionomycin treatment as described in Materials and Methods. The data represent the ratio acquired before ionomycin treatment subtracted from that obtained after ionomycin treatment.

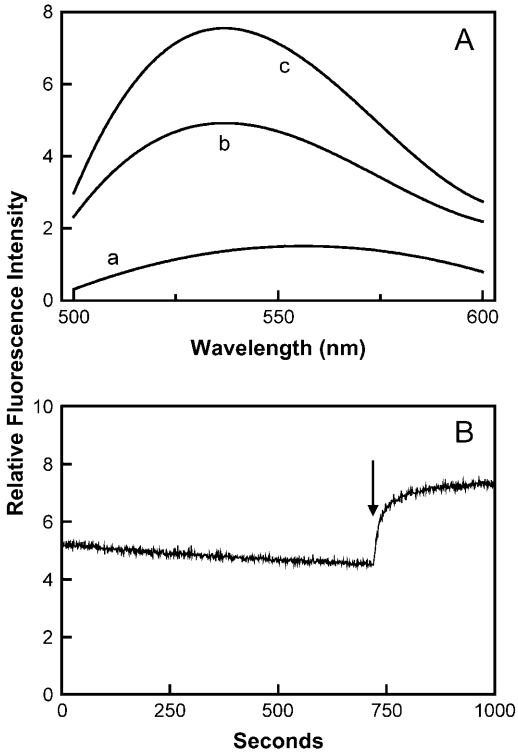

FIGURE 6 Effect of binding to BSA on fluorescence emission of NBD-PC at 37°C. (*A*) Fluorescence emission spectrum showing the intensity of an aqueous suspension of NBD-PC (*curve a*), erythrocytes labeled with NBD-PC (*curve b*, labeling details explained in Materials and Methods), and the same labeled cells after incubation with BSA (*curve c*). (*B*) Time course of fluorescence intensity of erythrocytes labeled with NBD-PC before and after addition of BSA (at the *arrow*).

analysis (see Materials and Methods). Fig. 8 illustrates a comparison in the kinetics of NBD-PC extraction from erythrocytes treated with ionomycin and those treated with the control diluent (DMSO). The more rapid rise in NBD fluorescence intensity observed in ionomycin-treated cells was reproducible (DMSO, $0.045 \pm 0.003\ s^{-1}$, ionomycin, $0.057 \pm 0.005\ s^{-1}$, $p = 0.04$, $n = 20$, paired *t*-test).

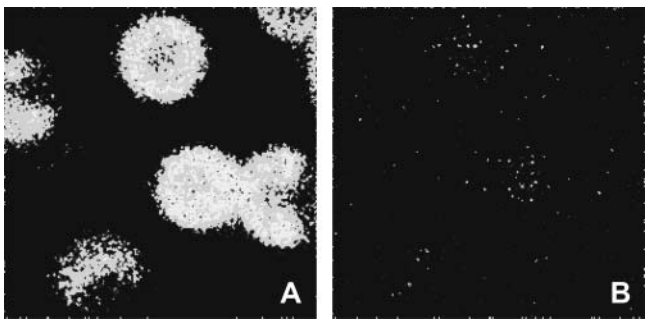

FIGURE 7 Extraction of NBD-PC from erythrocytes by BSA imaged by two-photon excitation microscopy. (*A*) Erythrocytes were labeled with NBD-PC as described in Fig. 6, and imaged by two-photon microscopy at 39°C. (*B*) An image of the same field was obtained again immediately after addition of BSA to the medium.

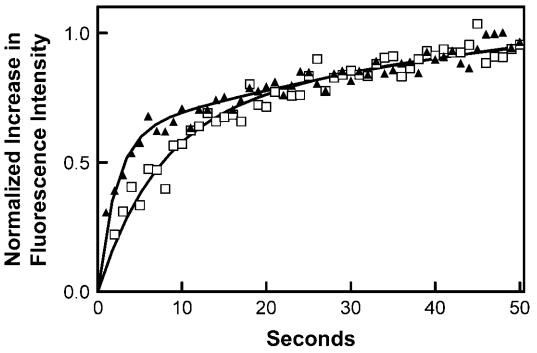

FIGURE 8 Effect of ionomycin on the initial rate of fluorescence intensity increase after addition of BSA. The experiment of Fig. 6 *B* was repeated with cells that had been incubated 10 min with either DMSO (*squares*) or ionomycin (*triangles*) before addition of BSA ($t = 0$). The fluorescence intensity before addition of BSA was subtracted, and the data were normalized to the intensity at 300 s.

Previous investigations identified a number of pharmacological manipulations that inhibit the various responses of erythrocytes to ionomycin and differ as to whether they also impair the effect of ionomycin to enhance susceptibility of the cells to $sPLA_2$ (Smith et al., 2001). The agents used were EDTA, R5421, high extracellular KCl, phenylhydrazine, and an inactive form of $sPLA_2$, AppK49. EDTA inhibits responses to ionomycin by chelating extracellular calcium and is therefore a useful control to identify whether observed responses are due to calcium flux as opposed to artifactual effects of the ionophore. R5421 inhibits scramblase (Dekkers et al., 1998), the calcium-activated transporter of phospholipids, but does not interfere with ionomycin-induced susceptibility to $sPLA_2$ (Smith et al., 2001). High extracellular KCl prevents the shedding of microvesicles from the plasma membrane in response to elevated intracellular calcium also without impeding membrane hydrolysis (Smith et al., 2001). In contrast, phenylhydrazine blocks ionomycin-induced susceptibility (Smith et al., 2001). AppK49 also inhibits the action of $sPLA_2$ (Wilson et al., 1999). However, instead of impairing the effect of intracellular calcium to alter membrane properties, AppK49 interferes with the adsorption of active $sPLA_2$ to the cell as explained above.

Fig. 9 illustrates the effects of these agents on the ability of ionomycin to enhance the rate of extraction of NBD-PC from erythrocytes by BSA. EDTA and phenylhydrazine repressed the extraction rate difference between ionomycin-treated cells and control samples. In contrast, neither high KCl nor R5421 impaired the effect of ionomycin. In fact, the average response appeared larger in the presence of R5421. Likewise, exposure of the cells to AppK49 had no effect on the rate of NBD-PC extraction by BSA in the presence of ionomycin.

As shown in Fig. 10, enhancement of the extraction rate by ionomycin was most obvious at temperatures in the range of 35−40°C ($p = 0.008$). At low temperatures, between 22

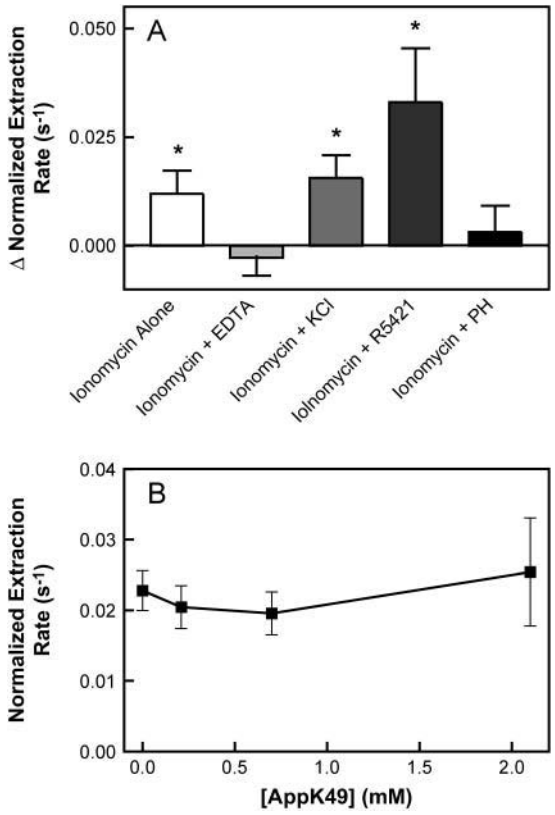

FIGURE 9 Effects of EDTA, R5421, KCl, phenylhydrazine, and K49 $sPLA_2$ on the ability of ionomycin to promote an increased rate of NBD-PC extraction. (*A*) Erythrocytes labeled with NBD-PC were incubated with these test agents before addition of ionomycin or DMSO as explained in Materials and Methods. NBD-PC extraction was assessed at least 5 min later upon addition of BSA and normalized as in Fig. 8. Data represent the arithmetic difference between samples treated with DMSO compared to those treated with ionomycin within each group. Statistics (paired *t*-tests comparing DMSO to ionomycin treatments assayed independently for each group)—EDTA, $p = 0.53$, $n = 8$; KCl, $p = 0.02$, $n = 8$; R5421, $p = 0.03$, $n = 8$; and Phenylhydrazine, $p = 0.61$, $n = 10$. (*B*) Erythrocytes labeled with NBD-PC were incubated 3 min with AppK49 (at the indicated concentrations) before addition of ionomycin. NBD-PC extraction was assessed at least 5 min later upon addition of BSA. No statistical differences among the data were observed based on analysis of variance ($p = 0.81$, $n = 10$–19).

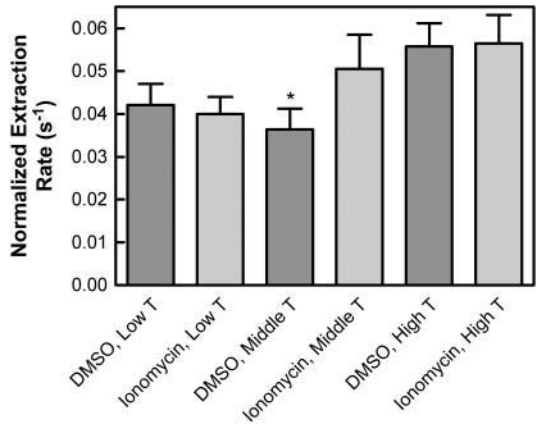

FIGURE 10 Rate of NBD-PC extraction by BSA with and without ionomycin at high, medium, and low temperatures. NBD-PC-labeled cells were incubated at various temperatures with and without ionomycin and then exposed to BSA as described in Materials and Methods. The data were quantified and normalized as in Fig. 8. (Trials were grouped into temperature categories as follows: *high*, 40–46°C; *medium*, 33–39.5°C; and *low*, 22–32°C.) Differences between ionomycin-treated and control groups were significant only in the medium temperature range (*$p = 0.008$, $n = 9$, paired *t*-test). Data represent mean ± SE.

and 33°C, the rate of phospholipid extraction was relatively slow for both ionomycin and DMSO treatments, and no difference between the groups was observed. Likewise, at high temperatures (41−48°C) there was also no significant difference in rate of phospholipid extraction between ionomycin and DMSO-treated erythrocytes, apparently because the rate in the control samples had reached that of samples treated with ionophore. In fact, the upward turn from the middle to the high temperature range was significant by linear regression ($p = 0.0003$; 37.5−48°C; $n = 14$). In contrast, no consistent trend was observed from 22 through 37°C ($p = 0.92$, $n = 19$). As expected from the results shown in Fig. 10, the effect of temperature across the entire range was statistically significant in the case of ionomycin treatment (22−37°C, $p = 0.04$, $n = 19$; 37.5−48°C, $p = 0.004$, $n = 15$).

Extraction of phospholipids by $sPLA_2$

If the results observed with BSA are relevant to enhancement of step 2 in the reaction scheme, one would expect the same behavior when $sPLA_2$ is used to extract NBD-PC, and that behavior should be reflective of the properties of the enzyme's active site. As shown in Fig. 11, when $sPLA_2$ was used as the phospholipid acceptor (squares, Fig. 11 *A*), similar changes in NBD intensity were observed although they were not as large and occurred more slowly than with BSA (Fig. 11 *B*). Replacement of calcium with barium (2 mM) in the extracellular medium resulted in an absence of change in NBD-PC fluorescence upon addition of $sPLA_2$ as demonstrated in Fig. 11 *A* (*triangles*), implying that no extraction had occurred. Under these conditions, barium occupies the active site of $sPLA_2$ and prevents formation of the ternary complex with phospholipid (Dam-Mieras et al., 1975; Yu et al., 1993a, 1998). Control experiments examining extraction by BSA in the presence of barium verified that the effect of barium shown in Fig. 11 was specific for $sPLA_2$. Thus, the inhibition of phospholipid extraction by barium argues that such extraction is directly relevant to the binding of substrate to the enzyme active site.

Secretory PLA_2 differs from BSA as an NBD-PC accepter because it adsorbs to the membrane surface rather than remaining free in solution and because it can hydrolyze the fluorescent phospholipid. To explore these issues, we examined NBD-PC extraction from erythrocytes by

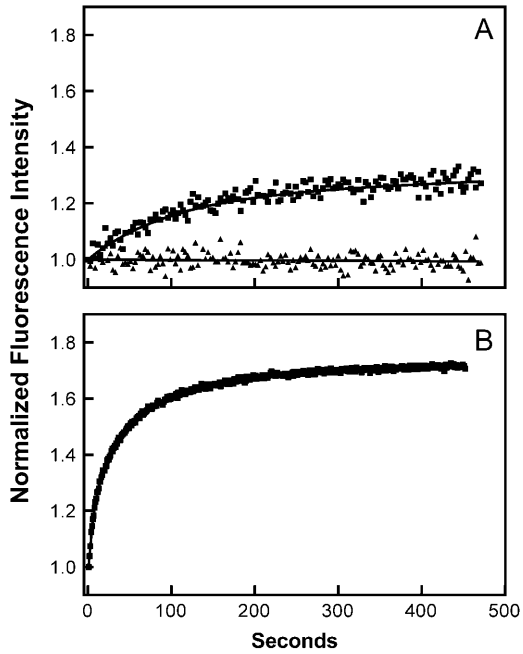

FIGURE 11 Migration of NBD-PC into the active site of $sPLA_2$ with calcium or with barium compared to NBD-PC extraction with BSA. (*A*) NBD-PC-labeled erythrocytes were prepared and incubated at 37°C in normal MBSS (1.6 mM $CaCl_2$, *squares*), or in low-calcium MBSS supplemented with $BaCl_2$ (2 mM, *triangles*). At time zero on the graph, $sPLA_2$ (70 nM) was added. (*B*) Display of data obtained as in Fig. 6 *B* for comparison purposes. BSA was added at time zero on the graph. In both *A* and *B*, the fluorescence intensity was normalized to the intensity of the first datum after addition of $sPLA_2$ or BSA.

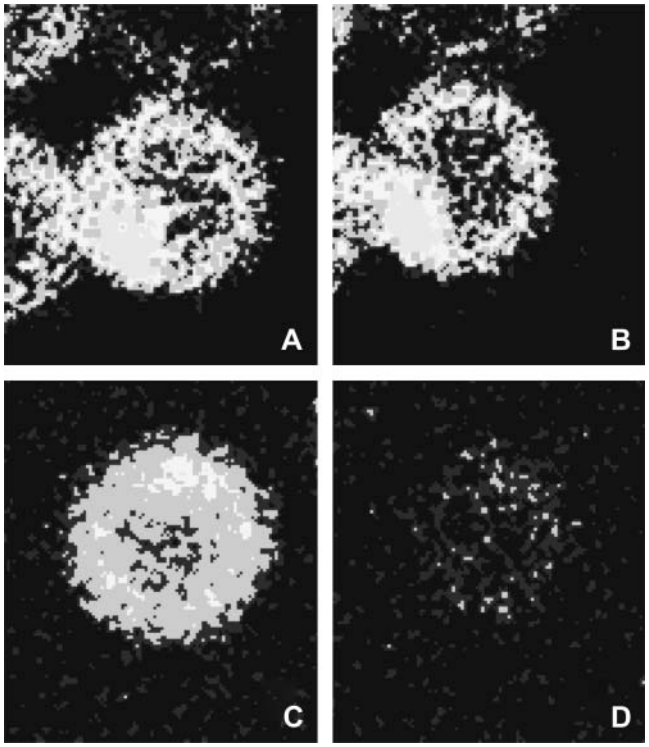

FIGURE 12 Two-photon microscopy images of the change in NBD-PC fluorescence in erythrocytes upon addition of $sPLA_2$. Images were collected as in Fig. 7. (*A*) Erythrocytes were treated 10 min with ionomycin at 25°C. (*B*) Same field as *A*, 3 min after $sPLA_2$ addition. (*C*) Erythrocyte treated 10 min with ionomycin at 42°C. (*D*) Same field as *C*, 3 min after $sPLA_2$ addition.

two-photon fluorescence microscopy. The assumption was that if the lipid were extracted by the enzyme but not hydrolyzed, the extensive loss of fluorescence from the membrane observed with BSA (Fig. 7) would not occur since the extracted lipid would remain bound to the enzyme on the membrane surface. Alternatively, hydrolysis produces NBD-labeled fatty acid which, due to its solubility in water, would diffuse away from the membrane, resulting in fluorescence loss. Fig. 12 demonstrates that incubation of the cells with $sPLA_2$ caused loss of NBD-PC from the cell membrane, indicating that hydrolysis was occurring. The extraction/hydrolysis took place over a time period from one to several min and was faster at higher temperature (compare Fig. 12, *C* and *D* to Fig. 12, *A* and *B*). Observation of the same field by light microscopy revealed that even though most or all of the NBD-PC was removed at the higher temperatures, the cells remained intact, suggesting that NBD-PC was a better substrate for $sPLA_2$ than the natural lipids.

We reasoned that the extraction and hydrolysis steps would be distinguishable in bulk samples since each step should cause opposite fluorescence changes upon addition of $sPLA_2$ to NBD-PC-labeled erythrocytes. The extraction step should result in enhanced NBD fluorescence because NBD-PC in the active site of $sPLA_2$ is protected from water and distanced from the autoquenching caused by other NBD-PC molecules (Nichols and Pagano, 1981). Upon hydrolysis, release of free NBD-fatty acid into the surrounding water would reduce its emission intensity due to quenching by the solvent. Thus, to quantify the effect of temperature on step two (Scheme 1) using $sPLA_2$, we assumed three possible states of NBD-PC molecules: NBD-PC intercalated in the membrane (L_m), NBD-PC bound to $sPLA_2$ (L_P), and NBD-PC that has been hydrolyzed (L_H). The other obvious compartment, NBD-PC free in solution, was assumed to be negligible. The fluorescence level (F) represents the sum of contributions from the various compartments,

$$F = F_0 L_m + F_P L_P + F_H L_H, \tag{10}$$

where F_0 is the initial fluorescence intensity when essentially all NBD-PC is still present in the membrane, F_P is the fluorescence intensity of NBD-PC bound to $sPLA_2$, and F_H is the fluorescence intensity of hydrolyzed NBD-PC. The various species of NBD-PC would be expressed as mole fractions. The differential equations describing the time-dependence are

$$\frac{dL_m}{dt} = -k_2 L_m \tag{11}$$

$$\frac{dL_P}{dt} = k_2 L_m - k_{cat} L_P. \quad (12)$$

The rate constants k_2 and k_{cat} represent the kinetics of extraction and hydrolysis, respectively. Integration of Eq. 11 followed by substitution into Eq. 12 and integration yields the following expressions for L_m and L_P:

$$L_m = L_{m(0)} e^{-k_2 t}, \quad (13)$$

$$L_P = \frac{k_2 L_{m(0)}}{k_{cat} - k_2}(e^{-k_2 t} - e^{-k_{cat} t}). \quad (14)$$

Since

$$L_H = L_{m(0)} - (L_m + L_P) \quad (15)$$

is due to conservation of mass, substitution of Eqs. 13–15 into Eq. 10 provides a complete expression for the NBD-PC fluorescence during extraction and hydrolysis by $sPLA_2$,

$$F = \alpha + \beta e^{-k_2 t} + \gamma(e^{-k_2 t} - e^{-k_{cat} t}), \quad (16)$$

where

$$\alpha = F_H L_{m(0)}$$
$$\beta = (F_0 - F_H) L_{m(0)}$$
$$\gamma = \frac{(F_P - F_H) k_2 L_{m(0)}}{(k_{cat} - k_2)}. \quad (17)$$

Fitting the data with Eq. 16 permitted calculation of the rate constant for extraction (k_2) and k_{cat} from a series of experiments at different temperatures (20–50°C) in which $sPLA_2$ was used as the NBD-PC acceptor (with α, β, and γ treated as arbitrary fitting constants). The value of k_2 was evaluated as a function of temperature by linear regression. As was true for the rate of extraction with BSA, k_2 increased with temperature in ionomycin-treated erythrocytes from 0.026 s^{-1} at 20°C to 0.055 s^{-1} at 47°C ($p = 0.04$, $n = 31$). The temperature trend for DMSO-treated samples was not significant ($p = 0.21$, $n = 31$). As expected (Best et al., 2002), the hydrolysis step (k_{cat}) also displayed significant temperature-dependence for both ionomycin-treated and control samples (undetectable at 20°C to 0.0004 s^{-1} at 47°C for ionomycin-treated samples, $p \leq 0.0007$ in both cases, $n = 31$).

DISCUSSION

This study was designed to test the hypothesis that physical changes in erythrocyte membrane structure induced by elevated intracellular calcium and temperature increase the susceptibility of that membrane to $sPLA_2$ by enhancing the second step in the reaction scheme (Scheme 1). The kinetic evidence (Figs. 1 and 2) strongly supported this hypothesis and argued that calcium loading and temperature combine to enhance hydrolysis by this mechanism. This argument predicted that measurements of enzyme adsorption isolated from the other steps in the reaction scheme should not reveal much dependence on either temperature or calcium loading. Although assessment of adsorption is difficult to interpret due to potential interaction with non-hydrolyzable sites on the membrane (Ancian et al., 1995; Koduri et al., 1998), the expected lack of temperature and ionomycin sensitivity was apparent. In contrast, the hypothesis predicted that both ionophore treatment and elevation in temperature should cause changes to the membrane representative of an increase in the ability of phospholipids to move vertically in the membrane. Assessment of lipid packing by MC540 fluorescence and extraction of NBD-PC provided evidence supporting the conclusion that ionomycin treatment combined with elevated temperature enhances the likelihood of vertical lipid migration. Thus, we conclude that induction of susceptibility in erythrocytes by calcium loading occurs by enhancing the second step in the reaction scheme.

A complexity in interpreting the data with NBD-PC was that the observed changes in extraction rates among the various experimental treatments were small compared to the changes anticipated from the kinetic data. The primary reason for this difficulty is the fact that NBD-PC is removed much more readily from the membrane than are native phospholipids. As shown in Fig. 7, all NBD-PC was removed quickly from labeled cells upon introduction of BSA. Since the cells remained intact during the extraction (based on light microscopy), we conclude that the extraction observed was preferential for NBD-labeled lipids. The increased mobility of these lipids seems consistent with the structure of NBD-PC since only one acyl chain inserts deeply into the bilayer. The other chain, attached to the NBD moiety, floats near the level of the glycerol backbone (Chattopadhyay, 1990). Nevertheless, the data of Figs. 8 and 9 illustrate that the effect of ionomycin was reproducible and consistent in each case with experimental conditions that do or do not allow susceptibility to $sPLA_2$.

The concept that the second step in Scheme 1 involves migration of phospholipid molecules from their normal position in the bilayer up into the active site of the bound enzyme originated from studies with model bilayers. Structural evaluation of $sPLA_2$ suggests that the active site of the adsorbed protein is not immersed in the bilayer (Scott et al., 1990). Hence, there is a physical displacement between the normal location of phospholipids in the membrane and their binding site in the enzyme. Furthermore, kinetic studies with polymerized lipids have indicated that catalysis is ineffective if phospholipids are constrained from being able to migrate upward from the plane of the bilayer (Wu and Cho, 1993; Soltys et al., 1993). Functional analysis of the hydrolysis of artificial membranes in the presence of various perturbing agents has also demonstrated the need for two distinct steps leading up to lipid catalysis (Burack and Biltonen, 1994; Yu et al., 1993b; Jain et al., 1989; Henshaw et al., 1998).

The proposal that step two would be the determining distinction between resistant and susceptible cell membranes was based on previous experiments with a fluorescent

membrane probe, laurdan. Those studies showed that ionomycin-induced susceptibility corresponds to an increase in the order of membrane lipids (Smith et al., 2001). However, subsequent experiments in which temperature was varied demonstrated that membrane order could not be the sole determining factor because an increase in order caused by lowered temperature resulted in reduced rather than enhanced hydrolysis by $sPLA_2$ (Best et al., 2002). Microscopic observations revealed a fundamental difference between adjusting membrane order with temperature or with ionomycin treatment. Temperature altered the membrane properties *homogeneously*, whereas the ionophore increased order *heterogeneously*. When ionomycin was added to the cells, the original membrane properties relevant to the experimental temperature were retained for much of the membrane, and domains of ordered lipids were superimposed on that background. Thus, when temperature was $>\sim 35°C$, ionomycin treatment produced sharp boundaries between ordered and disordered membrane regions. Further increases in temperature generated more heterogeneity and thus more and sharper domain boundaries. These effects appeared relevant to the action of $sPLA_2$ since membranes were most vulnerable to hydrolysis upon addition of ionomycin at elevated temperature (Fig. 2 and Best et al., 2002).

The MC540 data were useful in validating this interpretation. MC540 fluorescence is sensitive to the degree of lipid packing in the membrane (Langner and Hui, 1993; Lagerberg et al., 1995; Stillwell et al., 1993; Yu and Hui, 1992). Increasing membrane order homogeneously corresponds to tighter packing as observed in artificial membranes in the gel phase (Verkman, 1987; Langner and Hui, 1993; Bernik and Disalvo, 1993). In contrast, a heterogeneous increase in order creates a more complex effect on lipid packing because the ordering effect would promote packing whereas the proliferation of boundaries would diminish packing. Thus, total MC540 fluorescence observed for the sample would represent a balance between these two phenomena. If our hypothesis is correct, the heterogeneous ordering produced by calcium loading would increase packing at low temperature where the membrane is already ordered. Alternatively, the sharp boundaries formed at high temperature in the presence of ionophore could result in a net decrease in packing if the size of the domains is small and the number of boundaries therefore numerous. As shown in Fig. 5, these predicted results are exactly what were observed.

An alternative explanation that cannot be excluded by existing data pertains to transbilayer rather than horizontal heterogeneity in the membrane. Laurdan equilibrates across the membrane and therefore would report properties of both bilayer faces. The observed fluorescence would be the average of the two. Recent evidence argues that the effect of intracellular calcium on membrane order may involve direct binding of the cation to the interior of the cell membrane (Vest et al., 2004). This effect would cause ordering of the lipids on the inner face of the membrane resulting in a unilateral decrease in membrane surface area. This event would create strain on the outer face of the membrane since it would try to match surface area with the inner leaflet. MC540 would be preferentially exposed to this putative strain since it does not cross the cell membrane readily and would therefore bind only on the outer leaflet. This hypothetical strain could also account for the increased extraction and hydrolysis of fluorescent phospholipids since vertical migration of the lipids would be one way of relieving this strain.

We propose that these results and interpretations reached here with the simple membranes of erythrocytes apply to the more complex bilayers of nucleated cells. Calcium loading of various leukocyte cell lines also causes them to become susceptible to $sPLA_2$; in fact, the degree of gain in hydrolysis is much greater than observed in erythrocytes (Wilson et al., 1999). Physiologically, this phenomenon appears significant since cell membranes also become susceptible to the enzyme early during hormone-stimulated apoptosis (Nielson et al., 2000; Atsumi et al., 1997). Moreover, many of the phenomena relevant to this report have also been observed with human groups IIA and V $sPLA_2$ (Wilson et al., 1999; Smith et al., 2001). Accordingly, we propose that the simple hypothesis examined here applies broadly to describe the ability of $sPLA_2$ to distinguish healthy and damaged cell membranes.

Nevertheless, we do not intend to argue that step two is the only limiting step for all $sPLA_2$ species toward all healthy cell membranes. Calcium entry during cell injury causes exposure of the anionic phosphatidylserine in many cell types similar to that observed during apoptosis (Bevers et al., 1996). For many $sPLA_2$ isoforms, such exposure of anionic lipids can make a large difference in adsorption affinity (Jain et al., 1989; Henshaw et al., 1998; Koduri et al., 1998; Beers et al., 2003). This appears to be especially true for the human group IIA enzyme. Recent evidence suggests that it does not adsorb to the cell membrane unless phosphatidylserine has been exposed on the outer leaflet of the cell membrane (Koduri et al., 1998; Beers et al., 2003). In contrast, the ability of the human group V and snake venom enzymes to distinguish resistant and susceptible membranes is unaffected by pharmacological inhibition of phosphatidylserine exposure (Smith et al., 2001). Furthermore, it appears that protein receptors for $sPLA_2$ can also offer protection against the enzyme (Ancian et al., 1995). Given the obvious importance of protecting healthy cell membranes from the hydrolytic action of extracellular $sPLA_2$, it seems reasonable that multiple protective mechanisms would exist. We conclude that the results described here require that another mechanism be added to the list. Future experiments will address the relative importance of step two toward nucleated cells and with the various human enzymes.

Two-photon scanning microscopy experiments were performed at the Laboratory for Fluorescence Dynamics, Urbana, Illinois; gratitude is expressed

to Drs. Theodore Hazlett, Susana Sanchez, and Enrico Gratton for providing technical assistance and access to the facility for these experiments.

We also thank the Honors Program Office at Brigham Young University and Bioflam (University of Utah) for support of students working on this project. Finally, we acknowledge the assistance of Richard Jensen for assistance with acquisition of blood samples.

REFERENCES

Ancian, P., G. Lambeau, and M. Lazdunski. 1995. Multifunctional activity of the extracellular domain of the M-type (180 kDa) membrane receptor for secretory phospholipases A_2. *Biochemistry*. 34:13146–13151.

Arni, R. K., and R. J. Ward. 1996. Phospholipase A_2—a structural review. *Toxicon*. 34:827–841.

Atsumi, G., M. Murakami, M. Tajima, S. Shimbara, N. Hara, and I. Kudo. 1997. The perturbed membrane of cells undergoing apoptosis is susceptible to type II secretory phospholipase A_2 to liberate arachidonic acid. *Biochim. Biophys. Acta*. 1349:43–54.

Beers, S. A., A. G. Buckland, N. Giles, M. H. Gelb, and D. C. Wilton. 2003. Effect of tryptophan insertions on the properties of the human group IIA phospholipase A_2: mutagenesis produces an enzyme with characteristics similar to those of the human group V phospholipase A_2. *Biochemistry*. 42:7326–7338.

Bell, J. D., and R. L. Biltonen. 1989. Thermodynamic and kinetic studies of the interaction of vesicular dipalmitoylphosphatidylcholine with *Agkistrodon piscivorus piscivorus* phospholipase A_2. *J. Biol. Chem*. 264: 225–230.

Bernik, D. L., and E. A. Disalvo. 1993. Gel state surface properties of phosphatidylcholine liposomes as measured with merocyanine 540. *Biochim. Biophys. Acta*. 1146:169–177.

Best, K., A. Ohran, A. Hawes, T. L. Hazlett, E. Gratton, A. M. Judd, and J. D. Bell. 2002. Relationship between erythrocyte membrane phase properties and susceptibility to secretory phospholipase A_2. *Biochemistry*. 41:13982–13988.

Bevers, E. M., P. Comfurius, and R. F. Zwaal. 1996. Regulatory mechanisms in maintenance and modulation of transmembrane lipid asymmetry: pathophysiological implications. *Lupus*. 5:480–487.

Bezzine, S., J. G. Bollinger, A. G. Singer, S. L. Veatch, S. L. Keller, and M. H. Gelb. 2002. On the binding preference of human groups IIA and X phospholipases A_2 for membranes with anionic phospholipids. *J. Biol. Chem*. 277:48535–48549.

Burack, W. R., and R. L. Biltonen. 1994. Lipid bilayer heterogeneities and modulation of phospholipase A_2 activity. *Chem. Phys. Lipids*. 73: 209–222.

Chattopadhyay, A. 1990. Chemistry and biology of *n*-(7-nitrobenz-2-oxa-1,3-diazol-4-yl)-labeled lipids: fluorescent probes of biological and model membranes. *Chem. Phys. Lipids*. 53:1–15.

Dam-Mieras, M. C., A. J. Slotboom, W. A. Pieterson, and G. H. de Haas. 1975. The interaction of phospholipase A_2 with micellar interfaces. The role of the N-terminal region. *Biochemistry*. 14:5387–5394.

Dekkers, D. W., P. Comfurius, W. M. Vuist, J. T. Billheimer, I. Dicker, H. J. Weiss, R. F. Zwaal, and E. M. Bevers. 1998. Impaired Ca^{2+}-induced tyrosine phosphorylation and defective lipid scrambling in erythrocytes from a patient with Scott syndrome: a study using an inhibitor for scramblase that mimics the defect in Scott syndrome. *Blood*. 91:2133–2138.

Evans, E., and Y. C. Fung. 1972. Improved measurements of the erythrocyte geometry. *Microvasc. Res*. 4:335–347.

Gelb, M. H., M. K. Jain, A. M. Hanel, and O. G. Berg. 1995. Interfacial enzymology of glycerolipid hydrolases: lessons from secreted phospholipases A_2. *Annu. Rev. Biochem*. 64:653–688.

Harris, F. M., S. K. Smith, and J. D. Bell. 2001. Physical properties of erythrocyte ghosts that determine susceptibility to secretory phospholipase A_2. *J. Biol. Chem*. 276:22722–22731.

Heerklotz, H., and R. M. Epand. 2001. The enthalpy of acyl chain packing and the apparent water-accessible apolar surface area of phospholipids. *Biophys. J*. 80:271–279.

Henshaw, J. B., C. A. Olsen, A. R. Farnbach, K. H. Nielson, and J. D. Bell. 1998. Definition of the specific roles of lysolecithin and palmitic acid in altering the susceptibility of dipalmitoylphosphatidylcholine bilayers to phospholipase A_2. *Biochemistry*. 37:10709–10721.

Honger, T., K. Jorgensen, R. L. Biltonen, and O. G. Mouritsen. 1996. Systematic relationship between phospholipase A_2 activity and dynamic lipid bilayer microheterogeneity. *Biochemistry*. 35:9003–9006.

Jain, M. K., and O. G. Berg. 1989. The kinetics of interfacial catalysis by phospholipase A_2 and regulation of interfacial activation: hopping versus scooting. *Biochim. Biophys. Acta*. 1002:127–156.

Jain, M. K., B. Z. Yu, and A. Kozubek. 1989. Binding of phospholipase A_2 to zwitterionic bilayers is promoted by lateral segregation of anionic amphiphiles. *Biochim. Biophys. Acta*. 980:23–32.

Judd, A. M., K. B. Best, K. Christensen, G. M. Rodgers, and J. D. Bell. 2003. Alterations in sensitivity to calcium and enzymatic hydrolysis of membranes from sickle cell disease and trait erythrocytes. *Am. J. Hematol*. 72:162–169.

Koduri, R. S., S. F. Baker, Y. Snitko, S. K. Han, W. Cho, D. C. Wilton, and M. H. Gelb. 1998. Action of human group IIa secreted phospholipase A_2 on cell membranes. Vesicle but not heparinoid binding determines rate of fatty acid release by exogenously added enzyme. *J. Biol. Chem*. 273: 32142–32153.

Lagerberg, J. W., K. J. Kallen, C. W. Haest, J. VanSteveninck, and T. M. Dubbelman. 1995. Factors affecting the amount and the mode of merocyanine 540 binding to the membrane of human erythrocytes. A comparison with the binding to leukemia cells. *Biochim. Biophys. Acta*. 1235:428–436.

Langner, M., and S. W. Hui. 1993. Merocyanine interaction with phosphatidylcholine bilayers. *Biochim. Biophys. Acta*. 1149:175–179.

Maraganore, J. M., G. Merutka, W. Cho, W. Welches, F. J. Kezdy, and R. L. Heinrikson. 1984. A new class of phospholipases A_2 with lysine in place of aspartate 49. Functional consequences for calcium and substrate binding. *J. Biol. Chem*. 259:13839–13843.

Meyuhas, D., S. Yedgar, M. Rotenberg, N. Reisfeld, and D. Lichtenberg. 1992. The use of C6-NBD-PC for assaying phospholipase A_2-activity: scope and limitations. *Biochim. Biophys. Acta*. 1124:223–232.

Nichols, J. W., and R. E. Pagano. 1981. Kinetics of soluble lipid monomer diffusion between vesicles. *Biochemistry*. 20:2783–2789.

Nielson, K. H., C. A. Olsen, D. V. Allred, K. L. O'Neill, G. F. Burton, and J. D. Bell. 2000. Susceptibility of S49 lymphoma cell membranes to hydrolysis by secretory phospholipase A_2 during early phase of apoptosis. *Biochim. Biophys. Acta*. 1484:163–174.

Richieri, G. V., and A. M. Kleinfeld. 1995. Continuous measurement of phospholipase A_2 activity using the fluorescent probe ADIFAB. *Anal. Biochem*. 229:256–263.

Scott, D. L., S. P. White, Z. Otwinowski, W. Yuan, M. H. Gelb, and P. B. Sigler. 1990. Interfacial catalysis: the mechanism of phospholipase A_2. *Science*. 250:1541–1546.

Sieber, F. 1987. Merocyanine 540. *Photochem. Photobiol*. 46:1035–1042.

Singh, R. R., and J. Y. Chang. 2004. Investigating conformational stability of bovine pancreatic phospholipase A_2: a novel concept in evaluating the contribution of the ''native-framework'' of disulphides to the global conformational stability of proteins. *Biochem. J*. 377:685–692.

Smith, S. K., A. R. Farnbach, F. M. Harris, A. C. Hawes, L. R. Jackson, A. M. Judd, R. S. Vest, S. Sanchez, and J. D. Bell. 2001. Mechanisms by which intracellular calcium induces susceptibility to secretory phospholipase A_2 in human erythrocytes. *J. Biol. Chem*. 276:22732–22741.

Soltys, C. E., J. Bian, and M. F. Roberts. 1993. Polymerizable phosphatidylcholines: importance of phospholipid motions for optimum phospholipase A_2 and C activity. *Biochemistry*. 32:9545–9552.

Stillwell, W., S. R. Wassall, A. C. Dumaual, W. D. Ehringer, C. W. Browning, and L. J. Jenski. 1993. Use of merocyanine (MC540) in

quantifying lipid domains and packing in phospholipid vesicles and tumor cells. *Biochim. Biophys. Acta.* 1146:136–144.

Tatulian, S. A. 2001. Toward understanding interfacial activation of secretory phospholipase A_2 (PLA_2): membrane surface properties and membrane-induced structural changes in the enzyme contribute synergistically to PLA2 activation. *Biophys. J.* 80:789–800.

Udenfriend, S., S. Stein, P. Bohlen, W. Dairman, W. Leimgruber, and M. Weigele. 1972. Fluorescamine: a reagent for assay of amino acids, peptides, proteins, and primary amines in the picomole range. *Science.* 178:871–872.

Verkman, A. S. 1987. Mechanism and kinetics of merocyanine 540 binding to phospholipid membranes. *Biochemistry.* 26:4050–4056.

Vest, R. S., L. J. Gonzales, S. A. Permann, E. Spencer, L. D. Hansen, A. M. Judd, and J. D. Bell. 2004. Divalent cations increase lipid order in erythrocytes and susceptibility to secretory phospholipase A_2. *Biophys. J.* 86:2251–2260.

Williamson, P., A. Kulick, A. Zachowski, R. A. Schlegel, and P. F. Devaux. 1992. Ca^{2+} induces transbilayer redistribution of all major phospholipids in human erythrocytes. *Biochemistry.* 31:6355–6360.

Wilson, H. A., J. B. Waldrip, K. H. Nielson, A. M. Judd, S. K. Han, W. Cho, P. J. Sims, and J. D. Bell. 1999. Mechanisms by which elevated intracellular calcium induces S49 cell membranes to become susceptible to the action of secretory phospholipase A_2. *J. Biol. Chem.* 274:11494–11504.

Wu, S. K., and W. Cho. 1993. Use of polymerized mixed liposomes to study interactions of phospholipase A_2 with membranes. *Biochemistry.* 32:13902–13908.

Yu, B. Z., O. G. Berg, and M. K. Jain. 1993a. The divalent cation is obligatory for the binding of ligands to the catalytic site of secreted phospholipase A2. *Biochemistry.* 32:6485–6492.

Yu, B. Z., O. G. Berg, and M. K. Jain. 1993b. The divalent cation is obligatory for the binding of ligands to the catalytic site of secreted phospholipase A2. *Biochemistry.* 32:6485–6492.

Yu, B. Z., M. J. Poi, U. A. Ramagopal, R. Jain, S. Ramakumar, O. G. Berg, M. D. Tsai, K. Sekar, and M. K. Jain. 2000. Structural basis of the anionic interface preference and k_{cat}* activation of pancreatic phospholipase A2. *Biochemistry.* 39:12312–12323.

Yu, B. Z., J. Rogers, G. R. Nicol, K. H. Theopold, K. Seshadri, S. Vishweshwara, and M. K. Jain. 1998. Catalytic significance of the specificity of divalent cations as *KS** and k_{cat}* cofactors for secreted phospholipase A_2. *Biochemistry.* 37:12576–12587.

Yu, H., and S. W. Hui. 1992. Merocyanine 540 as a probe to monitor the molecular packing of phosphatidylcholine: a monolayer epifluorescence microscopy and spectroscopy study. *Biochim. Biophys. Acta.* 1107:245–254.

Yu, W., P. T. So, T. French, and E. Gratton. 1996. Fluorescence generalized polarization of cell membranes: a two-photon scanning microscopy approach. *Biophys. J.* 70:626–636.